



Co-ligand effects in the catalytic activity of Pd(II)–NHC complexes

Andrew Dahao Yeung, Pearly Shuyi Ng, Han Vinh Huynh*

Department of Chemistry, National University of Singapore, 3 Science Drive 3, Singapore 117543, Singapore

ARTICLE INFO

Article history:

Received 15 July 2010

Received in revised form

10 August 2010

Accepted 12 August 2010

Available online 20 August 2010

Keywords:

N-Heterocyclic carbenes

Palladium

Co-ligands effects

Mizoroki–Heck coupling

Conjugate addition

Boronic acids

ABSTRACT

Three *cis*-chelating di-*N*-heterocyclic carbene palladium(II) complexes [PdX₂(diNHC)] (X = I, **1**; X = SCN, **2**; X = CF₃CO₂, **3**) bearing different anionic co-ligands were synthesized and fully characterized. A comparison of their catalytic activities in the Mizoroki–Heck reaction and conjugate addition of arylboronic acids to cyclic enones revealed increasing efficiency in the order SCN[−] < I[−] < CF₃CO₂[−]. The di(trifluoroacetato) complex **3** showed the best activity in both transformations highlighting the importance of co-ligands effects in catalysis. In addition, the molecular structure of an unusual poly-hetero-nuclear complex salt **4** is reported, which has been isolated as a byproduct in the synthesis of complex **3**.

© 2010 Published by Elsevier B.V.

1. Introduction

The use of *N*-heterocyclic carbenes (NHCs) as ligands in organometallic chemistry is nowadays well established [1,2]. NHC ligands are generally stronger donors [3] compared to phosphines and have found applications as phosphine substitutes in Pd-mediated reactions including carbon–carbon bond formations [4], which are key synthetic steps in a variety of industrial processes [5]. These ligands have several advantages over the commonly utilized phosphines: (i) The strong σ -donating ability of NHCs, coupled with its minimal π -back bonding capabilities results in strong stabilizing effects and resistance to dissociation from the Pd center; (ii) the strong Pd–NHC bond and limited catalyst decomposition pathways ensures high thermal stability of Pd–NHC complexes, hence allowing for their use as catalyst at higher temperatures to increase reaction rates. Compared to monodentate NHCs, chelating dicarbene are expected to be more stable as the reductive elimination of carbene, a possible decomposition pathway, should take place at a slower rate for conformationally restricted systems. The importance of ancillary ligands in the design of transition metal catalysts is well established. On the other hand, the influence of co-ligands –beyond that of simple halides– on the catalytic activities has been less studied [6–8]. Herein, we report the synthesis and structural characterization of three *cis*-chelating dicarbene Pd(II) complexes bearing different anionic co-ligands and a comparison of

their catalytic activities in the conjugate addition of arylboronic acids to cyclic enones and the Mizoroki–Heck reaction. In addition, we report the unusual molecular structure of a poly-heteronuclear complex salt that has been isolated as a byproduct.

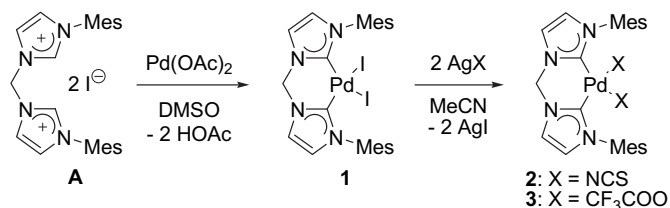
2. Results and discussion

2.1. Synthesis and characterization

The preparation of the palladium(II)–diNHC complexes is summarized in Scheme 1. Diiodo-(1,1'-dimesityl-3,3'-methyleneimidazolin-2,2'-diylidene)palladium(II) (**1**) was straightforwardly synthesized by *in situ* deprotonation of the imidazolium salt precursor (**A**) with palladium acetate in DMSO. A base peak at $m/z = 617$ for the [M – I]⁺ complex fragment in the positive mode ESI mass spectrum indicates formation of a carbene complex. The ¹H NMR spectrum of the yellow complex **1** shows generally broad ligand signals and geminal coupling of the methylene bridge was not resolved due to the fluxional behavior of the boat-shaped six-membered palladacycle [9].

Reaction of the air-stable complex **1** with the appropriate silver salts gave the analogous di(isothiocyanato) (**2**) and di(trifluoroacetato) (**3**) derivatives via a metathesis reaction [10]. To the best of our knowledge, **2** is the first reported mixed NHC–di(isothiocyanato) Pd(II) complex. These two complexes were isolated as white and air-stable solids. Even in DMSO solutions, they remain stable and did not decompose to give palladium black after prolonged standing. The successful replacement of the anionic co-

* Corresponding author. Tel.: +65 6516 2670; fax: + 65 6779 1691.



Scheme 1. Synthesis of Palladium(II)–NHC Complexes 1–3.

which has previously been observed for diphosphine analogues [12,13] and dicarbene–nickel(II) complexes [14].

2.2. Molecular structures

Single crystals of complex **1** and **3** were obtained easily by the slow diffusion of diethyl ether into a saturated acetonitrile solution, while single crystals of complex **2** were obtained from the slow diffusion of diethyl ether into a saturated DMF solution. Selected

Table 1
Selected bond lengths (Å) and angles (°) for complexes 1–4.

	1	2 ·DMF	3 ·CH ₃ CN	4 ·2(CH ₃) ₂ CO
Pd(1)–C(1)	2.018(5)	1.997(4)	1.969(4)	1.977(6)
Pd(1)–C(14)	2.029(5)	1.967(4)	1.969(4)	1.967(6)
Pd(1)–I(1)	2.6465(6)	–	–	–
Pd(1)–I(2)	2.6380(6)	–	–	–
Pd(1)–N(5)	–	2.046(3)	–	–
Pd(1)–N(6)	–	2.032(4)	–	–
Pd(1)–O(1)	–	–	2.068(3)	2.082(4)
Pd(1)–O(3)	–	–	2.083(3)	2.069(4)
C(1)–Pd(1)–C(14)	86.60(2)	86.07(15)	86.18(16)	86.9(2)
C(1)–Pd(1)–I(1)	92.11(16)	–	–	–
C(1)–Pd(1)–N(5)	–	95.38(13)	–	–
C(1)–Pd(1)–O(1)	–	–	93.06(14)	95.1(2)
PdC ₂ X ₂ /NHC dihedral angle	47.5(2), 47.5(2)	32.0(1), 37.5(1)	31.2(1), 37.2(1)	26.0(2), 30.6(2)

ligands is supported by isotopic envelopes in the ESI mass spectra of **2** and **3** at $m/z = 548$ for $[M - SCN]^+$ and 604 for $[M - CF_3CO_2]^+$, respectively. Furthermore, substitution of the iodo ligands in complex **1** with isothiocyanato ligands (**2**) decreased the complex's solubility in DMSO, whereas substitution by trifluoroacetate ligands (**3**) had the opposite effect [8,11].

The ¹H NMR spectra of complexes **2** and **3** agree with the expected structures. Similar to that of **1**, they exhibit broad signals, and the expected diastereotopy of the methylene bridge protons was not observed. Due to the limited solubility of all complexes **1–3** in most organic solvents including DMSO, we were unable to obtain well-resolved ¹³C NMR spectra despite prolonged acquisition time. As expected, the ¹⁹F NMR spectrum of **3** shows a singlet at 2.75 ppm for the trifluoroacetate ligands [6].

Finally, we did not observe any spectroscopic evidence for the formation of cationic (dicarbene) palladium(II) species as a consequence of autoionization or ligand disproportionation,

bond parameters are summarized in Table 1, and some important crystallographic data are listed in Table 2. Complexes **1–3** (Figs. 1–3) were crystallized as mononuclear complexes, in which the palladium center is coordinated by the chelating dicarbene ligand and two other co-ligands in an essentially square planar geometry (sum of angles around Pd is 359.33° for **1**, 360.21° for **2** and 360.34° for **3**). The dihedral angles between the NHC and PdC₂X₂ coordination planes are markedly smaller in complexes **2** and **3** compared to those in **1**, which is likely due to the increasing steric bulk of the anionic co-ligands. In all three complexes, the dicarbene bite angles are approximately 86°. This deviation from the perfect 90° angle may be due to the short methylene bridge. However, it has also been demonstrated that the length of flexible alkyl bridges has almost no effect on such dicarbene bite angles, but would significantly influence the dihedral angle between the NHC and coordination planes instead [14,15]. The averaged Pd–carbene bonds of complexes **2** [1.982(4) Å] and **3** [1.969(4) Å] are

Table 2
Selected X-ray crystallographic data for complexes 1–4.

	1	2 ·DMF	3 ·CH ₃ CN	4 ·2(CH ₃) ₂ CO
Formula	C ₂₅ H ₂₈ I ₂ N ₄ Pd	C ₃₀ H ₃₅ N ₇ OPdS ₂	C ₃₁ H ₃₁ F ₆ N ₅ O ₄ Pd	C ₇₉ H ₈₆ Ag ₂ F ₂₁ N ₈ O ₁₉ Pd ₂
Formula weight	744.71	680.17	758.01	2386.97
Color	Yellow	Colorless	Colorless	Orange
Temperature (K)	296(2)	100(2)	90(2)	223(2)
Crystal size (mm)	0.70 × 0.10 × 0.04	0.76 × 0.14 × 0.08	0.60 × 0.12 × 0.08	0.10 × 0.06 × 0.04
Crystal system	Orthorhombic	Monoclinic	Monoclinic	Monoclinic
Space group	P2 ₁ 2 ₁ 2 ₁	P2 ₁ /c	P2 ₁ /c	C2/c
<i>a</i> (Å)	7.6244(9)	13.1304(14)	12.9184(7)	16.7465(15)
<i>b</i> (Å)	13.6590(14)	16.3002(17)	16.1789(8)	18.9407(18)
<i>c</i> (Å)	25.328(3)	14.6497(16)	15.7207(8)	30.621(3)
α (°)	90	90	90	90
β (°)	90	90.869(2)	93.1840(10)	100.386(2)
γ (°)	90	90	90	90
<i>V</i> (Å ³)	2637.7(5)	3136.1(6)	3280.6(3)	9553.6(15)
<i>Z</i>	4	4	4	4
<i>D_c</i> (g cm ⁻³)	1.875	1.441	1.535	1.66
θ range (°)	1.61 to 27.48	1.55 to 27.50	1.58 to 27.50	1.64 to 25.00
Unique data	18819	19231	22942	8398
Final <i>R</i> indices [<i>I</i> > 2 σ (<i>I</i>)]	<i>R</i> ₁ = 0.0390, <i>wR</i> ₂ = 0.0833	<i>R</i> ₁ = 0.0515, <i>wR</i> ₂ = 0.1068	<i>R</i> ₁ = 0.0599, <i>wR</i> ₂ = 0.1166	<i>R</i> ₁ = 0.0588, <i>wR</i> ₂ = 0.1281

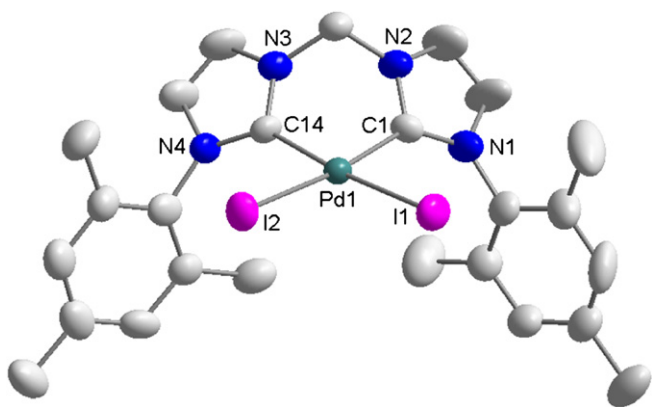


Fig. 1. Molecular structure of complex **1** showing 50% probability ellipsoids. Hydrogen atoms are omitted for clarity.

significantly shorter than that of the diiodo complex **1** [2.024(5) Å]. Similar reduced averaged Pd–C bond lengths (~1.9773 Å) were reported for the dicationic complex $[\text{Pd}(\text{CH}_3\text{CN})_2(\text{diNHC})](\text{PF}_6)_2$ bearing the same dicarbene ligand [16]. This is expected as the lower electron donating ability ($\text{I}^- > \text{NCS}^- > (\text{CH}_3\text{CN}) > \text{CF}_3\text{CO}_2^-$) of the trifluoroacetato and isothiocyanato ligands would induce a higher Lewis acidity on the palladium(II) center, which in turn leads to a higher electron donation of the dicarbene ligand to the metal center. This claim is further supported by the observation that the averaged Pd–carbene bond for the least donating di(trifluoroacetato) complex **3** is shorter in comparison to that of the di(isothiocyanato) complex **2**. Surprisingly, the overall charge of the complex seems to have less influence on the averaged Pd–carbene bonds compared to that of the co-ligands. The ambidentate isothiocyanato ligands in complex **2** are both coordinated through the hard N-atom with Pd–N distances of 2.046(3) Å and 2.032(4) Å, although the Pearson concept would predict an S-coordination to the soft Pd(II) center. This behavior can be explained by *anti-symbiosis*, which was defined as the preference of a hard donor *trans* to a soft donor bound to a soft metal center [17]. Nevertheless, it has been reported for diphosphine analogues that steric effects can enforce N- over S-coordination [18]. The Pd–O bonds in complex **3** are in the range reported for other mixed carbene–carboxylato Pd(II) complexes [6,10]. Further structural parameters are unexceptional and require no further comment.

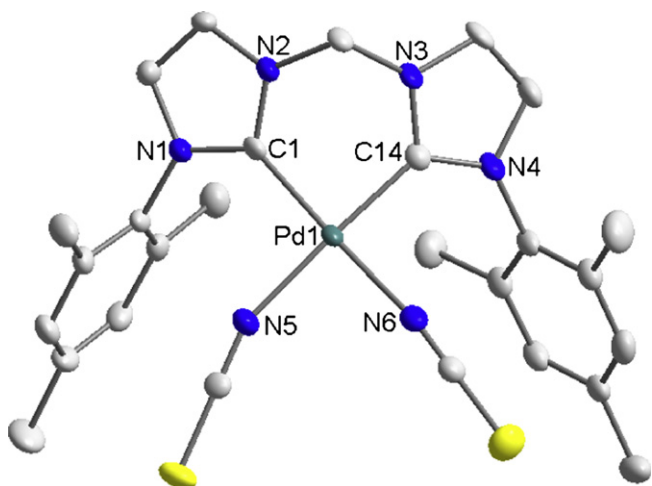


Fig. 2. Molecular structure of complex **2-DMF** showing 50% probability ellipsoids. Hydrogen atoms and the solvent molecule are omitted for clarity.

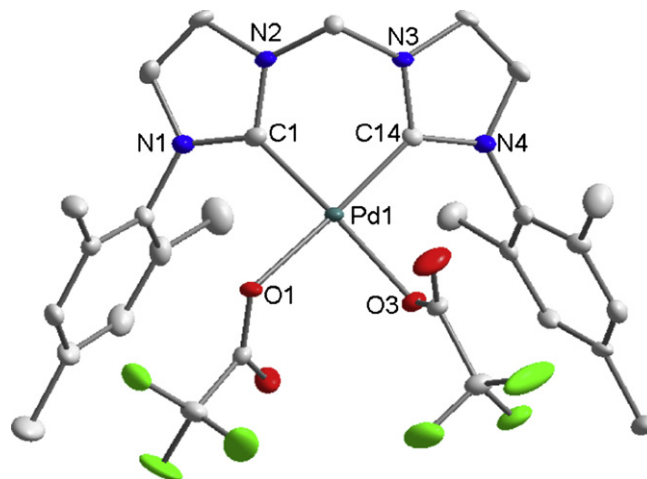


Fig. 3. Molecular structure of complex **3-CH₃CN** showing 50% probability ellipsoids. Hydrogen atoms and the solvent molecule are omitted for clarity.

Attempts to obtain single crystals from a crude mixture of complex **3** in acetone yielded a few single crystals of an unusual multinuclear byproduct **4** (Fig. 4), and its peculiar molecular structure determined by X-ray analysis is shown in Fig. 5.

Compound **4** can be described as a salt consisting of a heterotrimeric $[\text{Pd}_2\text{Ag}]$ -cation and a dinuclear $[\text{Ag}_2]$ -anion. The complex cation consists of two Pd(II)–dicarbene units that are both connected to one Ag(I) center through two bridging μ -trifluoroacetato ligands. The silver atom, which is also the center of inversion, is coordinated by four oxygen donors in a slightly distorted square planar geometry. Each of the palladium centers is coordinated by a *cis*-chelating dicarbene and two carboxylato ligands in a square planar fashion. The dicarbene bite angles [86.9(2)°], the palladium–carbene [1.967(6) and 1.977(6) Å] and the palladium–oxygen [2.082(4) and 2.069(4) Å] bond lengths are essentially the same as observed in complex **3**. However, the dihedral angle between the NHC and the PdC_2X_2 coordination planes has further decreased from **3** again due to increased steric crowding of the additional Ag-complex fragment. The silver–palladium separation is 2.8438(4) Å, which is significantly shorter than the sum of their van der Waals radii (3.35 Å). Nevertheless, the short distance is expected to be a result of the bridging trifluoroacetato ligands. More studies are required to reveal the true nature of such potential Pd–Ag interactions.

The dinuclear silver anion adopts a three-bladed propeller structure, with the trifluoroacetato ligands forming the blades about the hub comprising the two silver atoms and two terminally coordinated acetone molecules. The three blades with O–Ag–O bond angles of 94.0(3), 133.7(3), and 126.1(3)° are not spaced evenly apart. Each silver atom adopts a distorted trigonal bipyramidal structure. The inter-silver distance of 2.8415(11) Å is significantly shorter than the sum of their van der Waals radii (3.44 Å) suggesting a ligand-supported argentophilic interaction, which can

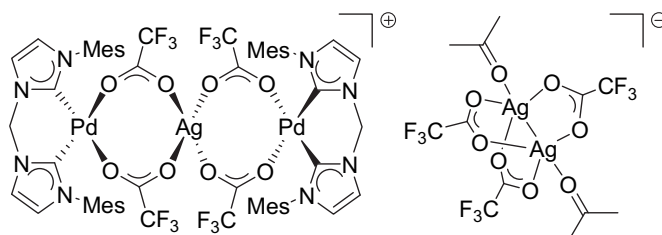


Fig. 4. Structural diagram of complex salt **4** (cation: left; anion right).

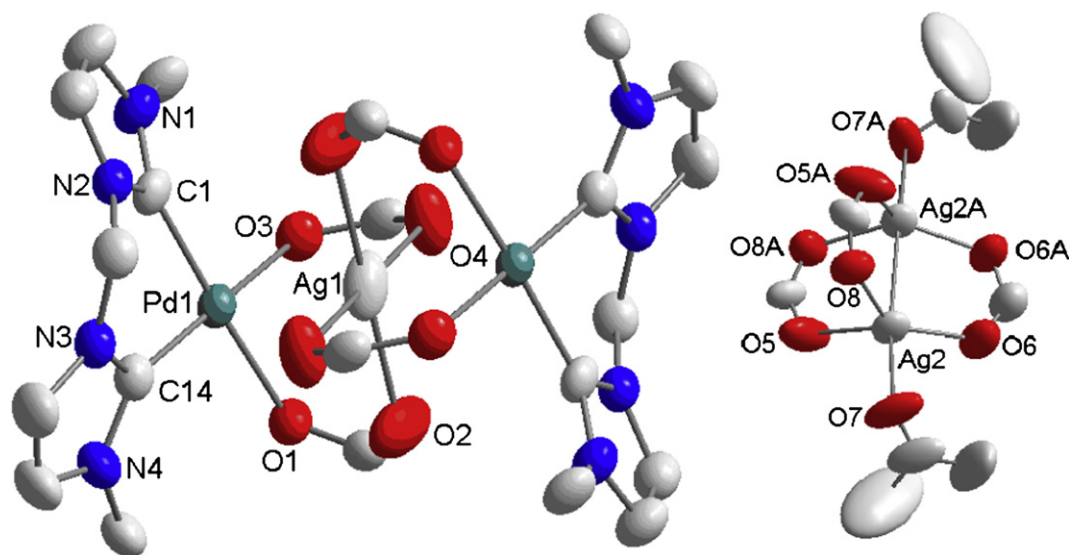


Fig. 5. Molecular structure of complex salt **4**·2(CH₃)₂CO (cation: left; anion right) showing 50% probability ellipsoids. Hydrogen atoms, solvent molecules and most atoms of the mesityl substituents are omitted for clarity.

also occur in the absence of supporting ligands [19,20], similar to the well-studied aurophilic interactions [21,22].

2.3. Mizoroki–Heck coupling reactions

A number of Pd(II) precatalysts with different of ancillary dicarbene ligands were investigated for their activities in the Mizoroki–Heck reaction and gave rise to high TONs for the coupling of aryl bromides [23,24]. In order to study any potential co-ligand effects on the catalytic activity, complexes **1–3** were also tested for their catalytic performance using this reaction. The coupling of simple aryl bromides and chlorides with *tert*-butyl acrylate in DMF at 1 mol% catalyst loading over 24 h was used as the standard test reaction.

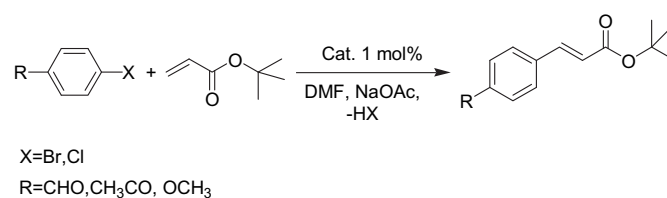
The results summarized in Table 3 indicate that all three complexes had some catalytic activity and in all instances the isothiocyanato complex **2** showed the lowest catalytic activity among the three complexes, while trifluoroacetato complex **3** consistently outperformed the diiodo complex **1** in the absence of any additives. The coupling of electron poor and activated substrates such as 4-bromobenzaldehyde and 4-bromoacetophenone at 120 °C (entries 1–6) proceeded with moderate to high yields, but the coupling of electron rich 4-bromoanisole resulted in no conversion for complexes **1** and **2**, and an only low yield of 16% for complex **3** (entry 9). Coupling of 4-chlorobenzaldehyde did not occur at 120 °C at all and gave only low yields with complexes **1** and **3** at 140 °C (entries 13 and 15). With the addition of [N(*n*-C₄H₉)₄]Br, the reaction yields were greatly improved (entries 19 and 21). However, the resulting excess of bromide anions also eliminated any observable co-ligand effects and catalyst precursor **1** and **3** gave essentially the same yield. Overall, the performance of complex **3** is slightly inferior to a related trifluoroacetato–Pd(II) complex bearing two monodentate benzimidazol-2-ylidenes under the same reaction conditions [6].

2.4. Conjugate addition of arylboronic acids to cyclic enones

Encouraged by the interesting co-ligand influence on the catalytic activities of the complexes exhibited in the Mizoroki–Heck coupling reaction, we explored the utility of the complexes in another catalytic system. Recent work reported by Shi et al. showed that chelating di(NHC)–palladium complexes bearing carboxylato ligands to be

effective catalysts in the conjugate addition of arylboronic acids to cyclic enones [25]. Hence, we set out to test the co-ligand effects using the synthesized complexes in this reaction. The results summarized in Table 4 indicate an even greater co-ligand effect in this reaction. Here only complex **3** was able to catalyze the reaction (entry 3) and in high yields. Complexes **1** and **2** were both ineffective (entries 1 and 2) in catalyzing the conjugate addition reaction and the phenylboronic acid was fully recovered. The addition of 4-biphenylboronic acid, 3- and 4-acetylbenzeneboronic acid using catalyst precursor **3** were equally effective giving high yields (entries 4–6). Surprisingly,

Table 3
Mizoroki–Heck Coupling reactions catalyzed by complexes **1–3**.^a



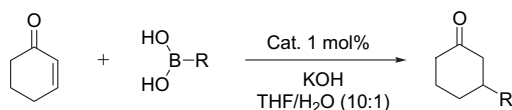
Entry	Catalyst	Aryl halide	Temp (°C)	Yield (%) ^b
1	1	4-Bromobenzaldehyde	120	89
2	2	4-Bromobenzaldehyde	120	85
3	3	4-Bromobenzaldehyde	120	97
4	1	4-Bromoacetophenone	120	79
5	2	4-Bromoacetophenone	120	57
6	3	4-Bromoacetophenone	120	>99
7	1	4-Bromoanisole	120	–
8	2	4-Bromoanisole	120	–
9	3	4-Bromoanisole	120	21
10	1	4-Bromotoluene	120	6
11	2	4-Bromotoluene	120	–
12	3	4-Bromotoluene	120	46
13	1	4-Chlorobenzaldehyde	140	8
14	2	4-Chlorobenzaldehyde	140	–
15	3	4-Chlorobenzaldehyde	140	15
16 ^c	1	4-Chlorobenzaldehyde	140	74
17 ^c	2	4-Chlorobenzaldehyde	140	–
18 ^c	3	4-Chlorobenzaldehyde	140	75

^a Reaction conditions generally not optimized.

^b Yields were determined by ¹H NMR spectroscopy over an average of two runs.

^c With addition of 1.5 equiv of [N(*n*-C₄H₉)₄]Br.

Table 4
Conjugate addition reactions catalyzed by complexes **1–3**.^a



Entry	Catalyst	R	Isolated yield (%) ^b
1	1		–
2	2		–
3	3		96 (97)
4	3		99 (97)
5	3		74
6	3		94
7	3		3
8	3		1

^a Reaction conditions generally not optimized.

^b Isolated yields over an average of two runs. () reported yield.[4].

3-nitrophenylboronic acid and thiophene-2-boronic acid failed to undergo conjugate addition indicating that substrates with donor atoms may deactivate the active species by coordination to the metal center (entries 7 and 8). The results obtained here clearly suggest a strong co-ligand influence in the conjugate addition of arylboronic acids to cyclic enones. Similar to the Mizoroki–Heck reaction, weakly coordinating carboxylate ligands play a very important role in the reaction allowing for an easy substrate binding and activation, whereas halido or pseudo-halido ligands are more difficult to be displaced leading to low activities.

3. Conclusion

Three *cis*-chelating di-*N*-heterocyclic carbene palladium(II) complexes [PdX₂(diNHC)] (X = I, **1**; X = SCN, **2**; X = CF₃CO₂, **3**) bearing different anionic co-ligands were synthesized and fully characterized. An interesting polynuclear complex salt (**4**) was obtained as a byproduct of in the synthesis of trifluoroacetato complex **3**. The identities of all complexes **1–4** have been confirmed by X-ray diffractions studies. Catalytic studies using the Mizoroki–Heck coupling reaction revealed a positive anionic co-ligand effect in the order of SCN[−] < I[−] < CF₃CO₂[−] for complexes of

the type [PdX₂(diNHC)]. The superiority of the di(trifluoroacetato) complex **3**, and thus the co-ligand effect, was even more pronounced for the catalytic conjugate addition of boronic acids to cyclohexenone, in which iodo and isothiocyanato complexes were completely inactive. These results highlight that the choice of co-ligand is equally important to that of the ancillary ligands and should not be neglected in catalyst design. Further work is underway to extend this study to other anions in order to establish a set of “privileged” co-ligands.

4. Experimental section

4.1. General considerations

All manipulations were carried out without taking precautions to exclude air and moisture unless otherwise stated. All solvents were used as received. ¹H and ¹⁹F NMR spectra were recorded on Bruker 300 MHz FT-NMR spectrometer at 300 and 282 MHz respectively. The residual protio-solvent or tetramethylsilane signals were used as the internal standard for ¹H NMR spectra; trifluoroacetic acid was used as the external standard for ¹⁹F NMR spectra. ¹³C NMR spectra were not obtained due to the poor solubility of the complexes. ESI mass spectra were obtained using a Finnigan MAT LCQ spectrometer. Elemental analyses were performed on a Perkin–Elmer PE 2400 elemental analyzer at the Department of Chemistry, National University of Singapore.

4.2. 1,1'-Dimesityl-3,3'-methylenediimidazolium diiodide (A)

Analogous to the previously-reported dibromide salt [9], 1-mesitylimidazole (1.50 g, 8.05 mmol, 2 equiv) was dissolved in toluene (10 mL) and diiodomethane (0.32 mL, 4.03 mmol, 1 equiv) was added. The resultant solution was heated at 150 °C for 48 h. The white precipitate was filtered off, washed with toluene and tetrahydrofuran (10 mL each), and dried *in vacuo*. Yield: 2.19 g (84%). ¹H NMR (300 MHz, DMSO-*d*₆): δ 9.76 (s, 2H, NCHN), 8.33 (s, 2H, CH), 8.10 (s, 2H, CH), 7.17 (s, 4H, Ar-H), 6.84 (s, 2H, NCH₂N), 2.34 (s, 6H, *p*-ArCH₃), 2.03 (s, 12H, *o*-ArCH₃). MS (ESI) *m/z* (%): 513 (60) [M – I]⁺.

4.3. Diiodo-(1,1'-dimesityl-3,3'-methylenediimidazolin-2,2'-diylidene)palladium(II) (**1**)

A mixture of **A** (1.40 g, 2.19 mmol, 1 equiv) and Pd(OAc)₂ (0.49 g, 2.19 mmol, 1 equiv) in DMSO (12 mL) was heated at 60 °C for 1 h, then 80 °C for 16 h to give a bright orange solution. The solvent was removed via vacuum distillation at 70 °C to afford a bright orange residue. Dichloromethane (10 mL) was added to the residue and the mixture was stirred and filtered. The bright yellow residue was washed with dichloromethane (2 × 10 mL), and dried *in vacuo*. Yield: 1.22 g (75%). ¹H NMR (300 MHz, DMSO-*d*₆): δ 7.90 (s, br, 2H, CH), 7.45 (s, br, 2H, CH), 7.02 (s, br, 4H, Ar-H), 6.56 (s, br, 2H, NCH₂N), 2.29 (s, br, 6H, *p*-ArCH₃), 2.02 (s, br, 12H, *o*-ArCH₃). MS (ESI) *m/z* (%): 617 (100) [M – I]⁺; 127 (93) [I][−].

4.4. Di(isothiocyanato)(1,1'-dimesityl-3,3'-methylenediimidazolin-2,2'-diylidene)palladium(II) (**2**)

A mixture of **1** (1.00 g, 1.34 mmol, 1 equiv) and silver thiocyanate (0.45 g, 2.68 mmol, 2 equiv) in acetonitrile (15 mL) was shielded from light and heated at 65 °C overnight to give a light yellow suspension. The mixture was filtered, and the white residue was washed with acetonitrile (20 mL). The white residue was further stirred with DMSO (20 mL) at room temperature overnight, and filtered again. Solvents were removed from the combined filtrates to give a white solid, which was washed with diethyl ether (20 mL)

and dried *in vacuo* to give the desired product. Yield: 0.52 g (64%). ^1H NMR (300 MHz, DMSO- d_6): δ 7.91 (s, 2H, CH), 7.50 (s, 2H, CH), 6.99 (s, 4H, Ar-H), 6.55 (s, 2H, NCH $_2$ N), 2.26 (s, 6H, *p*-ArCH $_3$), 1.96 (s, 12H, *o*-ArCH $_3$). MS (ESI) m/z (%): 548 (100) [M – SCN] $^+$; 58 (10) [SCN] $^-$.

4.5. 1,1'-Dimesityl-3,3'-methylenediimidazolin-2,2'-diylidene-di(trifluoroacetato)palladium(II) (3)

A mixture of **1** (2.418 g, 3.25 mmol, 1 equiv) and silver trifluoroacetate (1.43 g, 6.50 mmol, 2 equiv) in acetonitrile (30 mL) was shielded from light and heated to reflux overnight to give a grey-green precipitate in an orange solution. The solids were filtered off, and the orange filtrate was dried *in vacuo* to give an orange residue. The residue was suspended in dichloromethane (15 mL) and filtered to give the desired product as a white solid, which was washed with diethyl ether (20 mL) and dried. Yield: 1.39 g (60%). ^1H NMR (300 MHz, DMSO- d_6): δ 7.96 (s, 2H, CH), 7.50 (s, 2H, CH), 7.01 (s, br, 4H, Ar-H), 6.57 (s, 2H, NCH $_2$ N), 2.28 (s, 6H, *p*-ArCH $_3$), 2.01 (s, 12H, *o*-ArCH $_3$). ^{19}F NMR (282 MHz, DMSO- d_6): δ 2.75 (CF $_3$). MS (ESI) m/z (%): 548 (100) [M – SCN] $^+$; 604 (40) [M – CF $_3$ CO $_2$] $^+$; 113 (100) [CF $_3$ CO $_2$] $^-$.

4.6. General procedure for the Mizoroki–Heck reaction

A 15 mL reaction tube was charged with aryl halide (1 mmol), anhydrous sodium acetate (1.5 mmol), catalyst (0.01 mmol) and *N,N*-dimethylformamide (3 mL). The tube was sealed, heated to 120 °C, and *tert*-butyl acrylate (1.4 mmol) was added. No additional procedures were taken to prevent the ingress of atmospheric oxygen and moisture. After 24 h, the reaction was cooled, and dichloromethane (5 mL) was added. The organic phase was washed with water (5 \times 5 mL), dried with sodium sulfate, filtered, and dried *in vacuo*. The residue was analyzed by ^1H NMR spectroscopy, and conversion was calculated by comparing the integrals of the aryl halide starting material, and the Mizoroki–Heck product.

4.7. General procedure for conjugate addition of boronic acids to cyclic enones

The catalyst (0.03 mmol), potassium hydroxide (0.40 mmol), and THF (4 mL) were charged in a Schlenk tube and stirred under nitrogen for 10 min. Boronic acid (1.5 mmol), enone (1.00 mmol), and water (0.4 mL) were added sequentially, and the reaction mixture was stirred at room temperature for 36 h. Saturated aqueous sodium bicarbonate solution (5 mL) was added, and the organic phase was separated. The aqueous layer was extracted twice more with ethyl acetate (5 mL), and the combined organic layers were dried with sodium sulfate, filtered, and dried *in vacuo*. The crude material was chromatographed on silica-gel (30 \rightarrow 70% ethyl acetate in hexanes) to obtain the pure product.

4.8. X-ray diffraction studies

Suitable single crystals were mounted on glass fibers. X-ray data were collected with a Bruker AXS SMART APEX diffractometer, using Mo K α radiation, with the SMART suite of programs [26]. Data was processed and corrected for Lorentz and polarization effects with SAINT [27], and for absorption effect with SADABS [28]. Structural solution and refinement were carried out with the SHELXTL suite of

programs [29]. The structure was solved by direct methods to locate the heavy atoms, followed by difference maps for the light, non-hydrogen atoms. All hydrogen atoms were put at calculated positions. All non-hydrogen atoms were generally given anisotropic displacement parameters in the final model. A summary of the most important crystallographic data is given in Table 2.

Acknowledgements

The authors thank the National University of Singapore for financial support (Grant No. R 143-000-407-112) and especially Ms Geok Kheng Tan and Prof. Lip Lin Koh for determining the X-ray molecular structures.

Appendix A. Supplementary material

CCDC-783145 (for **1**), -783146 (for **2**·DMF), -783147 (for **3**·CH $_3$ CN), and -783148 (for **4**·2(CH $_3$) $_2$ CO) contain the supplementary crystallographic data for this paper. These data can be obtained free of charge from The Cambridge Crystallographic Data Centre via www.ccdc.cam.ac.uk/data_request/cif. Supplementary data associated with this article can be found, in the online version, at doi:10.1016/j.jorgchem.2010.08.017.

References

- [1] D. Bourissou, O. Guerret, F.P. Gabbai, G. Bertrand, Chem. Rev. 100 (2000) 39–91.
- [2] F.E. Hahn, M.C. Jahnke, Angew. Chem. Int. Ed. 47 (2008) 3122–3172.
- [3] H.V. Huynh, Y. Han, R. Jothibas, J.A. Yang, Organometallics 28 (2009) 5395–5404.
- [4] E.A.B. Kanchev, C.J. O'Brien, M.G. Organ, Angew. Chem. Int. Ed. 46 (2007) 2768–2813.
- [5] B. Cornils, W.A. Hermann, Applied Homogeneous Catalysis with Organometallic Compounds, second ed. VCH, Weinheim, 2002.
- [6] M.S. Viciu, E.D. Stevens, J.L. Petersen, S.P. Nolan, Organometallics 23 (2004) 3752–3755.
- [7] H.V. Huynh, T.C. Neo, G.K. Tan, Organometallics 25 (2006) 1298–1302.
- [8] H.V. Huynh, H.X. Seow, Aust. J. Chem. 62 (2009) 983–987.
- [9] W.A. Herrmann, M.G. Gardiner, C.-P. Reisinger, J. Schwarz, M. Spiegler, J. Organomet. Chem. 572 (1999) 239–247.
- [10] H.V. Huynh, D. Le Van, F.E. Hahn, T.S.A. Hor, J. Organomet. Chem. 689 (2004) 1766–1770.
- [11] Y. Han, H.V. Huynh, L.L. Koh, J. Organomet. Chem. 692 (2007) 3606–3613.
- [12] A. Marson, A.B.v. Oort, Wilhelmus P. Mul, Eur. J. Inorg. Chem. (2002) 3028–3031.
- [13] C. Bianchini, A. Meli, W. Oberhauser, Organometallics 22 (2003) 4281–4285.
- [14] H.V. Huynh, R. Jothibas, Eur. J. Inorg. Chem. (2009) 1926–1931.
- [15] F.E. Hahn, T. von Fehren, T. Lügger, Inorganica Chim. Acta 358 (2005) 4137–4144.
- [16] T. Scherg, S.K. Schneider, G.D. Frey, J. Schwarz, E. Herdtweck, W.A. Herrmann, Synlett 18 (2006) 2894–2907.
- [17] L. Battan, S. Fantasia, M. Manassero, A. Pasin, M. Sansoni, Inorganica Chim. Acta 358 (2005) 555–564.
- [18] G.J. Palenik, M. Mathew, W.L. Steffen, G. Beran, J. Am. Chem. Soc. 97 (1975) 1059–1066.
- [19] C.Y. Chen, J.Y. Zeng, H.M. Lee, Inorganica Chim. Acta 360 (2007) 21–30.
- [20] L. Ray, M.M. Shaikh, P. Ghosh, Inorg. Chem. 47 (2008) 230–240.
- [21] H. Schmidbaur, S. Cronje, B. Djordjevic, O. Schuster, Chem. Phys. 311 (2005) 151–161.
- [22] H. Schmidbaur, Nature 413 (2001) 31–33.
- [23] M.V. Baker, B.W. Skelton, A.H. White, C.C. Williams, J. Chem. Soc. Dalton Trans. (2001) 111–120.
- [24] C. Tubaro, A. Biffis, C. Gonzato, M. Zecca, M. Basato, J. Mol. Catal. A 248 (2006) 93–98.
- [25] T. Zhang, M. Shi, Chem. Eur. J. 14 (2008) 3759–3764.
- [26] SMART (Version 5.628). Bruker AXS Inc., Madison, WI, USA, 2001.
- [27] SAINT+ (Version 6.22a). Bruker AXS Inc., Madison, WI, USA, 2001.
- [28] G.W. Sheldrick, SADABS (Version 2.10). University of Göttingen, 2001.
- [29] SHELXTL (Version 6.14). Bruker AXS Inc., Madison, WI, USA, 2000.